Brown Carbon Fuel and Emission Source Attributions to Global Snow Darkening Effect

Hunter Brown[1,2], Hailong Wang[3], Mark Flanner[4], Xiaohong Liu[2], Balwinder Singh[3], Rudong Zhang[3], Yang Yang[5], Mingxuan Wu[3]

[1]Department of Atmospheric Science, University of Wyoming, Laramie, WY, USA.

[2]Department of Atmospheric Sciences, Texas A&M University, College Station, TX, USA.

[3]Atmospheric Sciences and Global Change Division, Pacific Northwest National Laboratory, Richland, WA, USA.

[4]Department of Atmospheric, Oceanic and Space Sciences, University of Michigan, Ann Arbor MI, USA

[5]Jiangsu Key Laboratory of Atmospheric Environment Monitoring and Pollution Control, Jiangsu Collaborative Innovation Center of Atmospheric Environment and Equipment Technology, School of Environmental Science and Engineering, Nanjing University of Information Science and Technology, Nanjing, Jiangsu, China

Contents of this file

Text S1 to S2
Figures S1 to S13
Tables S1 to S3

Introduction

The goal of this supplementary is to add additional information regarding the analyses presented in the main text. This includes the tabulated data and methods used when comparing model data to collected snow samples (in Fig. 2 in main text), the equation used for temporal cross correlation (in Fig. 10 in main text), a flow chart describing the incorporation of brown carbon (BrC) in SNICAR (in section 2.2.3 in main text), and additional plots that support the conclusions in the main text.

Observational data is collected from Doherty et al. (2010), Wang et al. (2013), and Doherty et al. (2014). All model comparisons are generated using the same CESM tagging implementation and brown carbon parameterization described in the main text. The GEOS-Chem model mass absorption cross section (MAC) is from Tuccella et al. (2021), while the brown carbon MAC are derived from a 1-year simulation for the year 2005. Other model analyses are based on the same three simulations described in the main text (i.e., BRC, BRC_PB, and NOBRC). These additional analysis include: the difference and ratio between BrC snow darkening effect (SDE) with different model treatments; source contributions to BrC SDE with photochemical bleaching; comparison of regional SDE and deposition for different light absorbing species; seasonal variation SDE and variables affecting SDE calculation; and the modeled sea-ice surface area in the Arctic and Antarctic.

Model Validation S1.

Model data is selected from grid cells and monthly time stamps that correspond to the collection dates and latitude-longitude of the observations. Modeled BC snow surface concentration (ng g^{-1}) from the BRC simulation is used to compare to C_{BC} (Fig. 2a). Due to the similarities between filter absorption measurements and the impact of absorbing aerosol on snow albedo, the ratio of modeled dust and OC SDE to total aerosol SDE (($SDE_{dust}+SDE_{OC}$)/(SDE_{aer})) is used as a comparison to f_{non-BC} (Fig. 2b). Samples were neglected in cases where there was no snow in the model corresponding to the sample dates in the observations (i.e., SDE = 0) and where underlying snow surfaces in the model were darkened to such a degree that $SDE_{dust}+SDE_{OC}$ or SDE_{aer} was negative (i.e., non-physical f_{non-BC}).

Cross-correlation Coefficient S2.

The following equation is used to calculate the Pearson sample linear cross-correlation coefficients at lag 0 (TCC) between BrC SDE (X) and the various mechanisms that impact calculation of BrC SDE (Y),

$$TCC = \frac{1}{N-1} \frac{\sum_{i=1}^{N}(X_i - \bar{X})(Y_i - \bar{Y})}{\sqrt{\frac{\sum_{i=1}^{N}(X_i - \bar{X})^2}{N-1}} \sqrt{\frac{\sum_{i=1}^{N}(Y_i - \bar{Y})^2}{N-1}}} = \frac{1}{N-1} \frac{\sum_{i=1}^{N}(X_i - \bar{X})(Y_i - \bar{Y})}{X_{std}Y_{std}}$$

Eq. S1

where N is months in the year, $\bar{X}$ is the annual mean BrC SDE, $\bar{Y}$ is the annual mean input to BrC SDE calculation, X_{std} is the standard deviation in monthly BrC SDE, and Y_{std} is the standard deviation in the monthly input to BrC SDE calculation.

References

Doherty, S. J., Warren, S. G., Grenfell, T. C., Clarke, A. D., & Brandt, R. E. (2010). Light-absorbing impurities in Arctic snow. *Atmos. Chem. Phys.*, *10*(23), 11647–11680. https://doi.org/10.5194/acp-10-11647-2010

Doherty, S. J., Dang, C., Hegg, D. A., Zhang, R., & Warren, S. G. (2014). Black carbon and other light-absorbing particles in snow of central North America: Black carbon in North American snow. *Journal of Geophysical Research: Atmospheres*, *119*(22), 12,807-12,831. https://doi.org/10.1002/2014JD022350

Wang, Xin, Doherty, S. J., & Huang, J. (2013). Black carbon and other light-absorbing impurities in snow across Northern China. *Journal of Geophysical Research: Atmospheres*, *118*(3), 1471–1492. https://doi.org/10.1029/2012JD018291
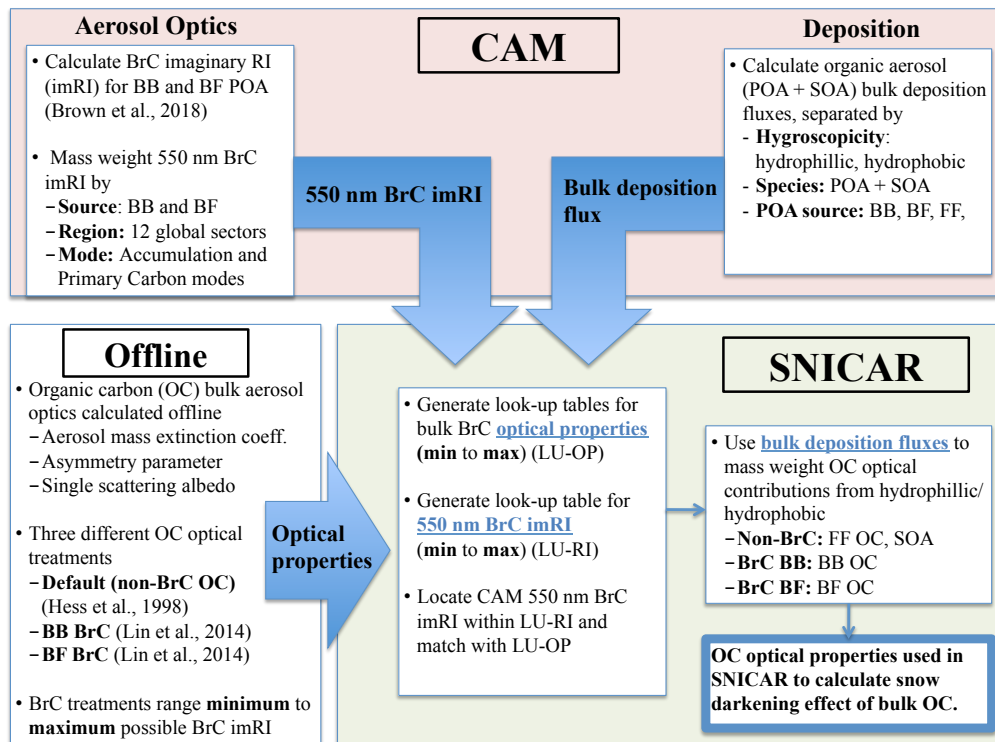
Figure S1. A visual depiction of the transfer of brown carbon (BrC) imaginary refractive index from the Community Atmosphere Model (CAM) to the Snow Ice and Aerosol Radiative (SNICAR) model within the Community Land Model (CLM).
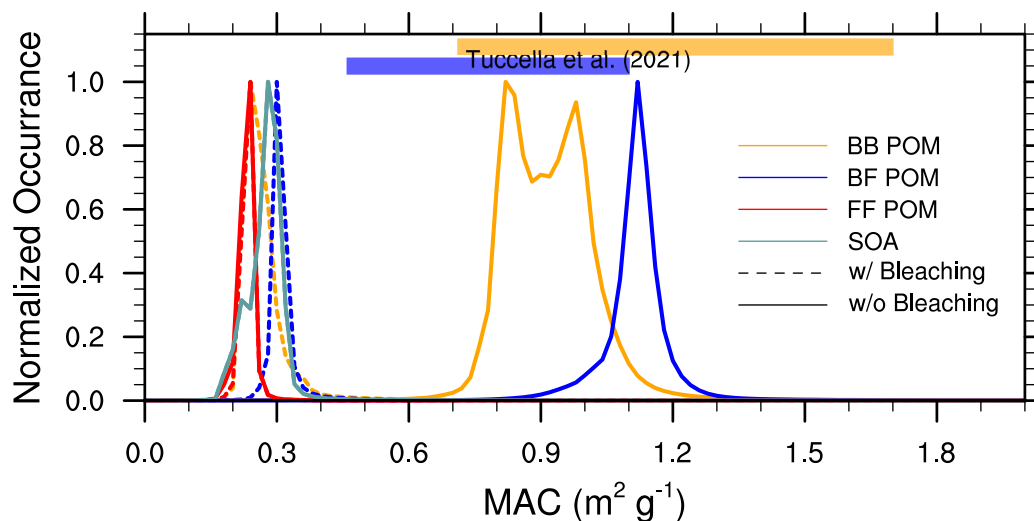

Figure S2. Mass absorption cross-section (MAC) of POM – both BrC and non-BrC – in CAM for the year 2005. The MAC are averaged over the visible spectrum (0.3-0.7 μm). Solid lines are from BRC simulations while dashed lines are from BRC_PB simulations. Prescribed BrC MAC from Tuccella et al. (2021),

from aged to fresh (left to right) are represented by solid bars at the top of the plot.
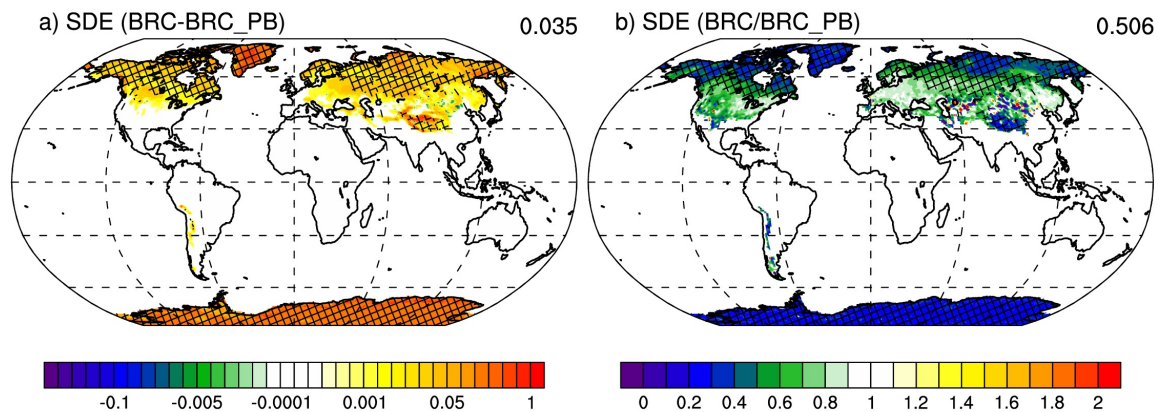

Figure S3. Global plot of the difference and ratio of BrC SDE. a) difference between BrC SDE from BRC and BRC_PB simulations (BRC-BRC_PB) and b) ratio of BrC SDE from BRC and BRC_PB simulations (BRC_PB/BRC). Hatching indicates grid cells where the change across the 10 simulation years is significant to the 0.1 level.
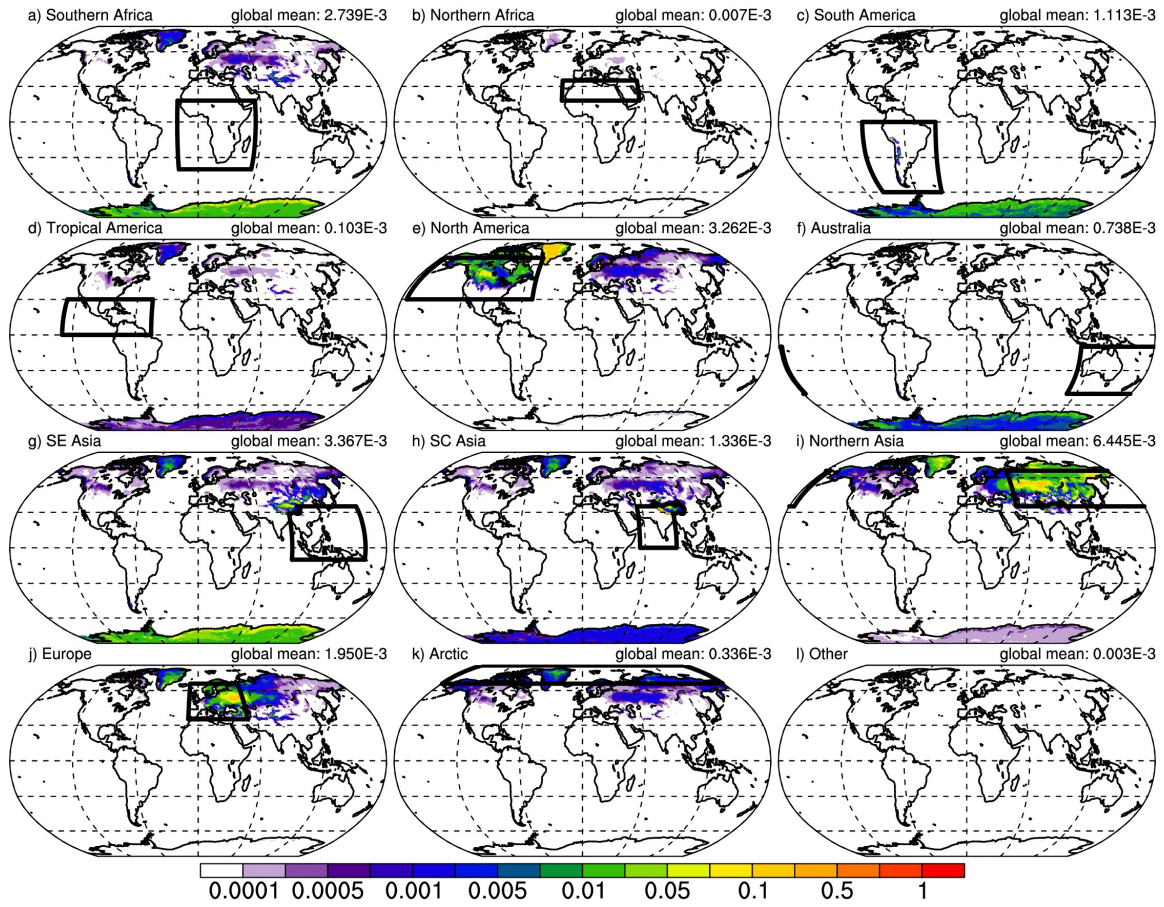
Figure S4. Regional contribution to the 10-year mean BrC snow darkening effect (SDE; W m⁻²) from BB and BF sources. The SDE is from the BRC_PB simulation (bleaching BrC) so represents the lower bound for BrC contribution to SDE. Emission regions are marked in each panel with a solid black box and correspond to the regions in Fig. 1. The BrC SDE is averaged over all grid-cells, with and without snow cover.
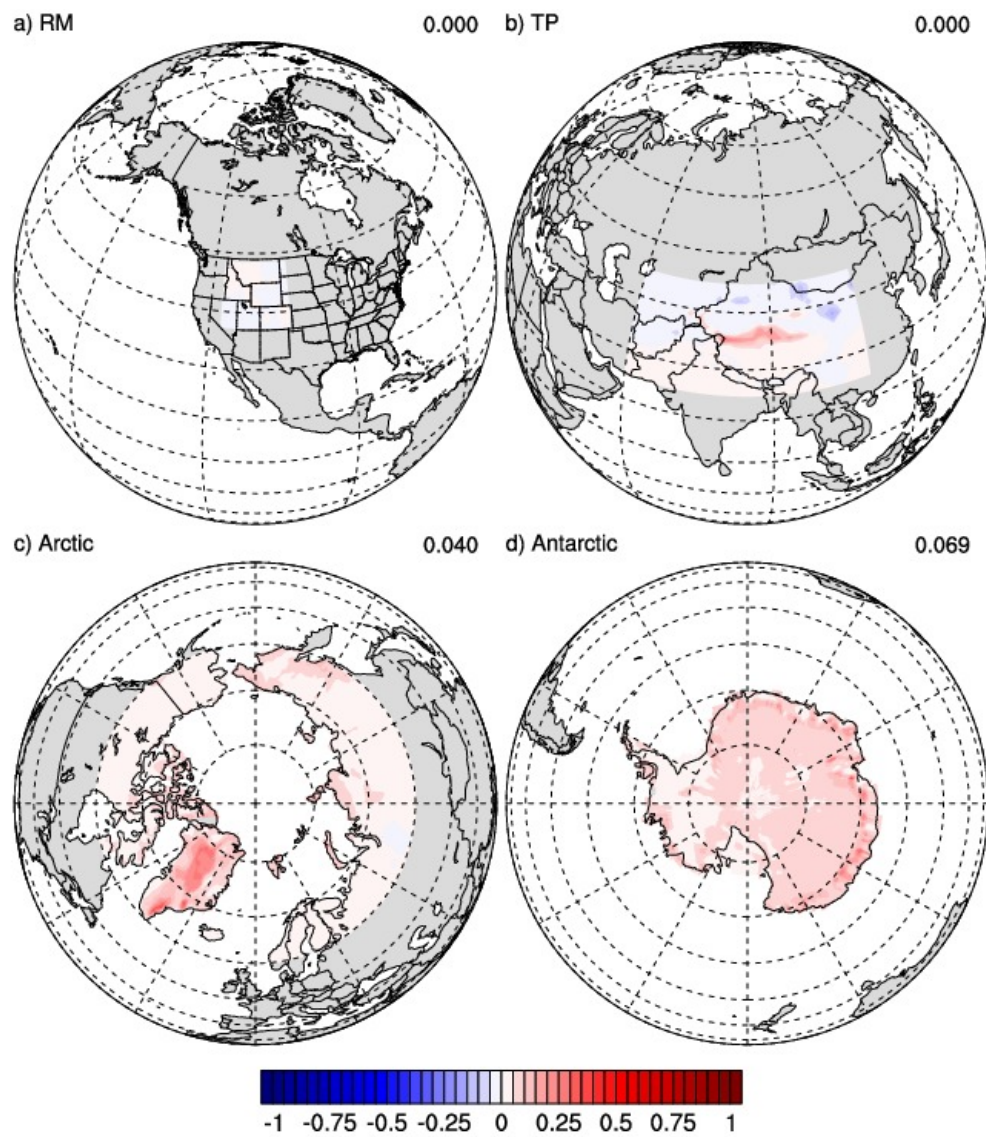
Figure S5. Same as Fig. 7 but showing SDE (W m^{-2}) from OC in the NOBRC simulation.

a) RM   34.268 b) TP   270.021

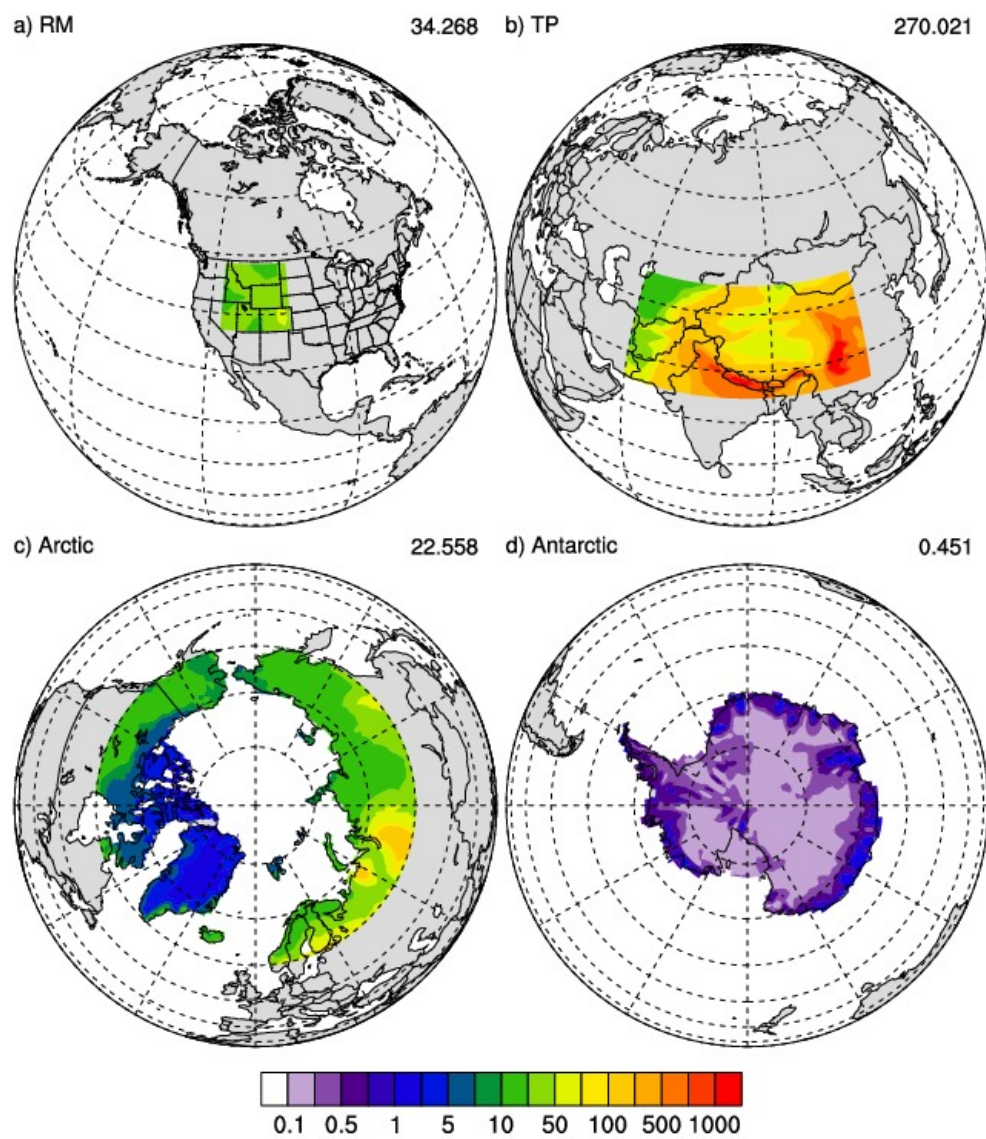c) Arctic   22.558 d) Antarctic   0.451

0.1 0.5 1 5 10 50 100 500 1000

Figure S6. Same as Fig. S4 but showing BC deposition (ug m^{-2} day^{-1}).

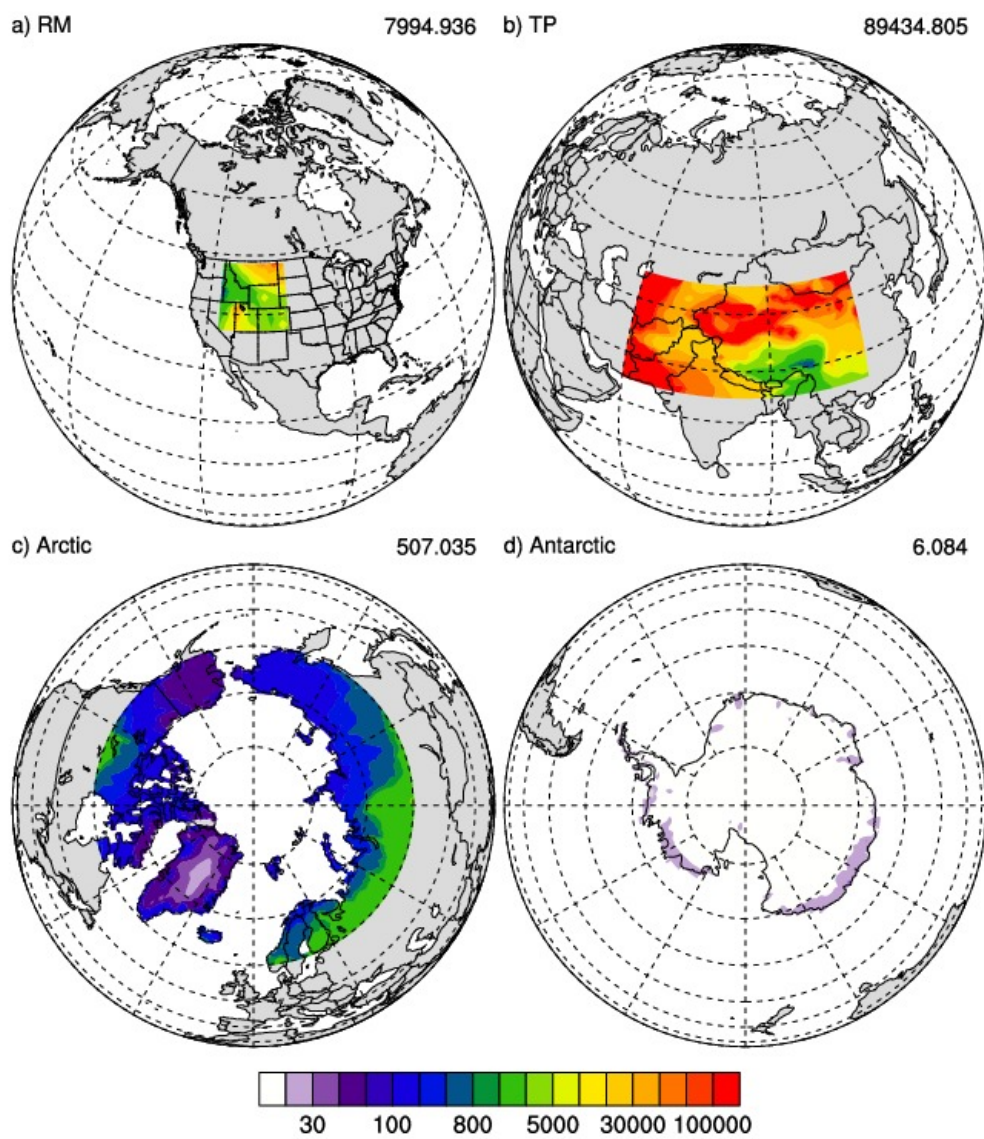**Figure S7.** Same as Fig. S5 but showing dust deposition (ug m⁻² day⁻¹). Note that the scale is increased 2 orders of magnitude from that of Fig. S5.
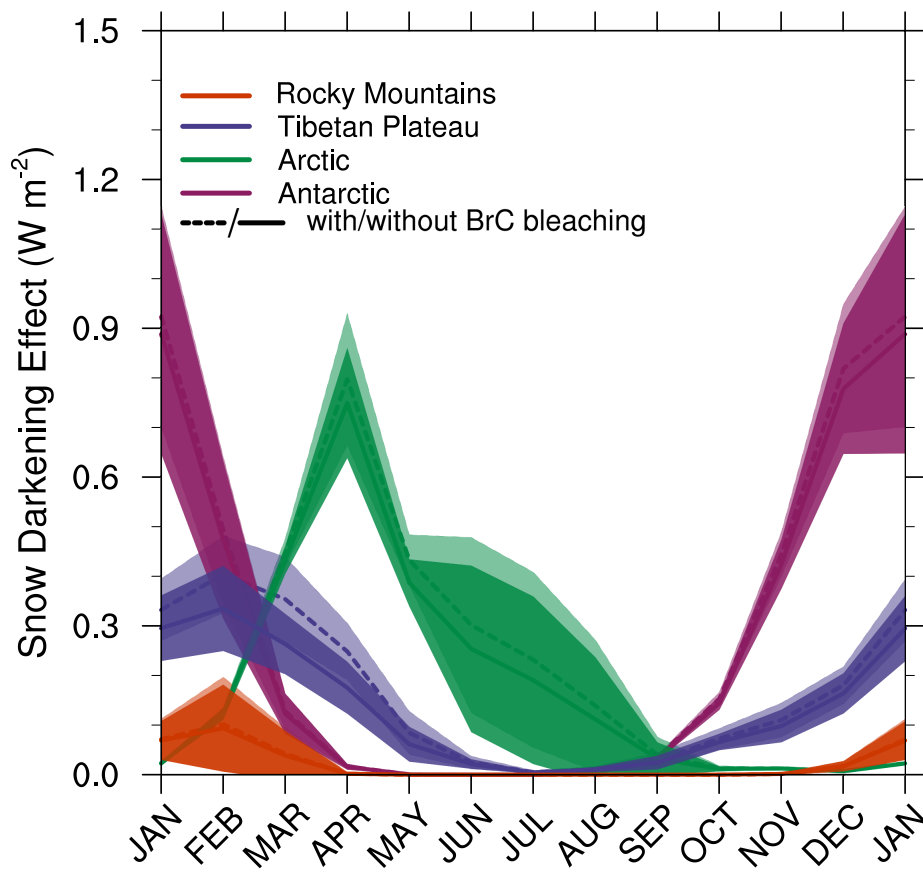
Figure S8. Monthly mean variation in 10-year mean BC + dust SDE (Wm⁻²) from the four regions described in Fig. 8, ± one standard deviation. Colors represent the Rocky Mountains (orange), the Tibetan Plateau (purple), the Arctic (green), and the Antarctic (maroon). The BC+dust SDE is from the BRC and BRC_PB simulations and is averaged over all grid-cells, with and without snow cover.
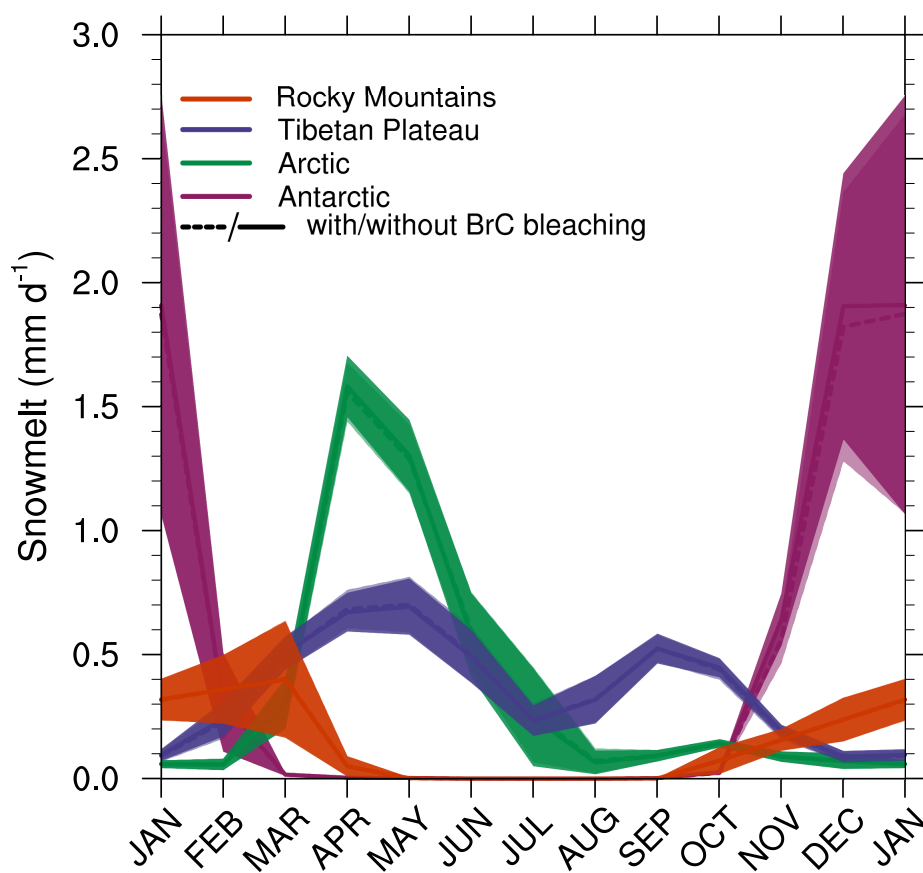
Figure S9. Monthly mean variation in 10-year mean snowmelt (mm d^{-1} from the four regions described in Fig. 8, ± one standard deviation. Colors represent the Rocky Mountains (orange), the Tibetan Plateau (purple), the Arctic (green), and the Antarctic (maroon). The snowmelt is from the BRC and BRC_PB simulations.

Figure S10. Temporal cross-correlation between monthly average BrC SDE and mechanisms that play into the calculation of SDE. These mechanisms are BB BrC deposition flux (kg m^{-2} s^{-1}), BF BrC deposition flux (kg m^{-2} s^{-1}), snow column organic carbon (kg m^{-2}), BC+dust SDE (W m^{-2}). All cycles are normalized for this comparison. Colors represent the Rocky Mountains (orange), the Tibetan Plateau (purple), the Arctic (green), and the Antarctic (maroon).

Figure S11. Monthly mean variation in 10-year mean snow cover fraction (%) from the four regions described in Fig. 8, ± one standard deviation. Colors represent the Rocky Mountains (orange), the Tibetan Plateau (purple), the Arctic (green), and the Antarctic (maroon). The snow cover fraction is from the BRC and BRC_PB simulations

Figure S12. Monthly mean variation in 10-year mean BB BrC deposition flux (ng m⁻² s⁻¹) from the four regions described in Fig. 8, ± one standard deviation. Colors represent the Rocky Mountains (orange), the Tibetan Plateau (purple), the Arctic (green), and the Antarctic (maroon). The deposition flux is from the BRC and BRC_PB simulations.
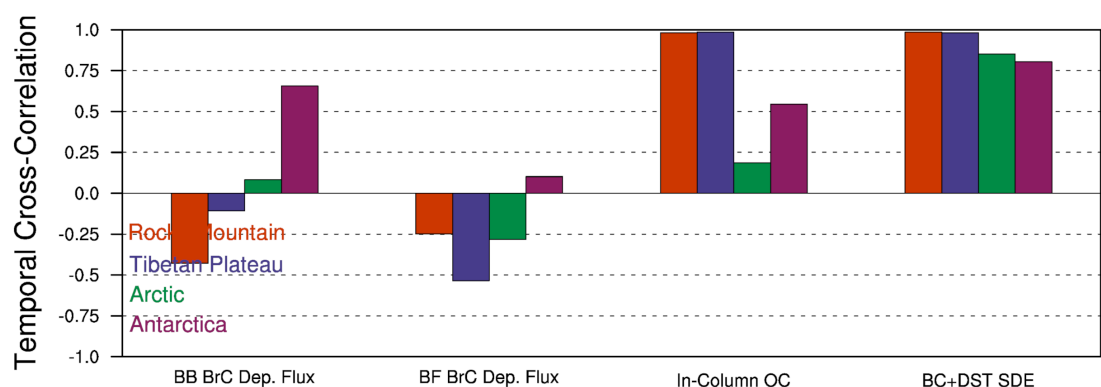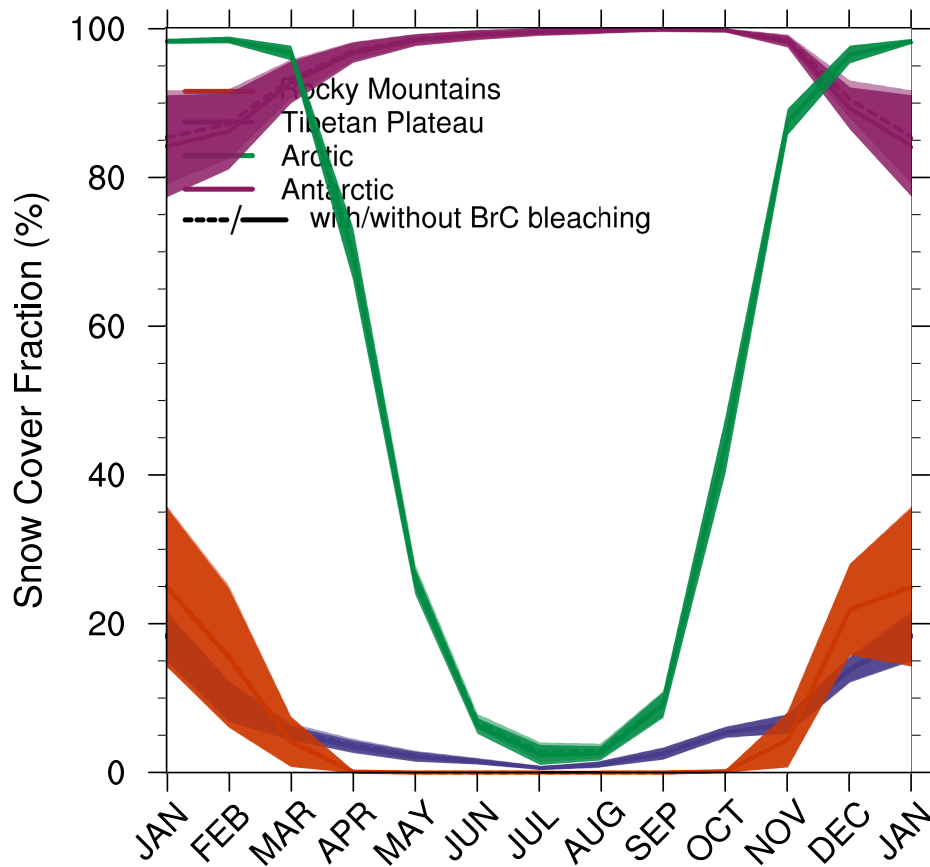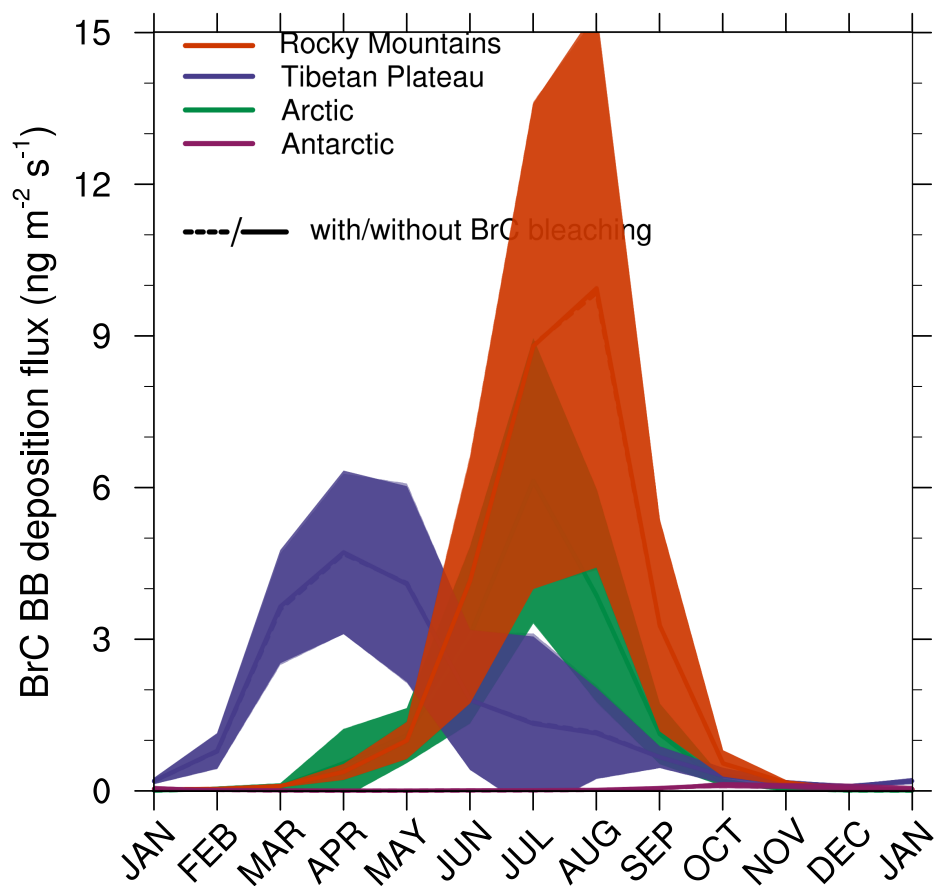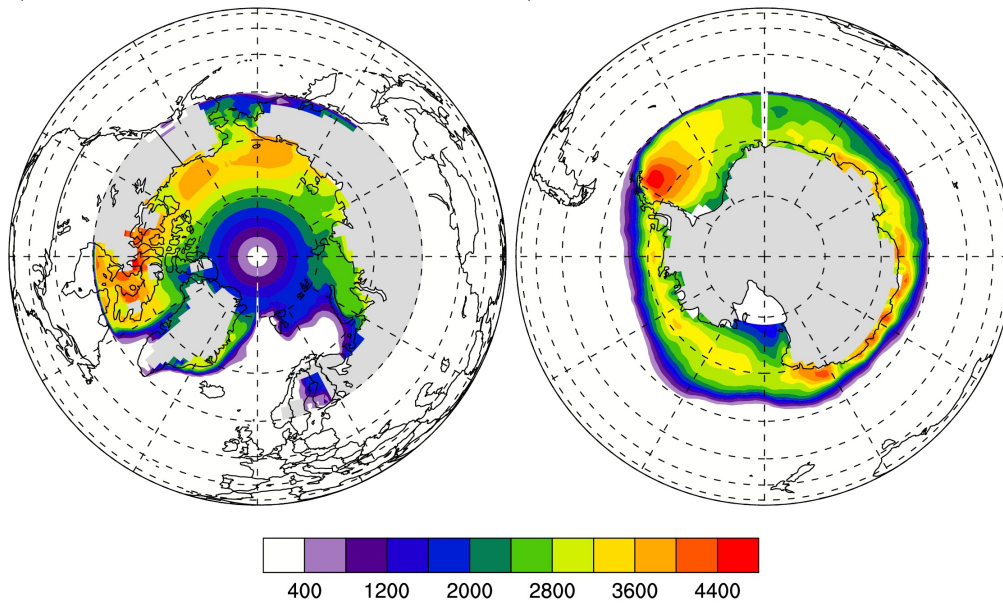
a) Arctic

b) Antarctic

400 1200 2000 2800 3600 4400

Figure S13. The 10-year mean sea-ice grid cell surface area (km^2) over (a) the Arctic and (b) the Antarctic.

	Observations	BRC
Canada and Alaska[a]		
Canadian Arctic	9.39±3.23	20.2±9.56
Canadian subarctic	15.42±8.64	24±7.73
N. Alaska Coast	9	54.14
Ellesmere Island	12	5.37
Greenland[a]		
South Greenland	1.1	–
Central Greenland	2	5.06
Northeast Greenland	7.53±10.88	–
Northwest Greenland	4.2	6.35
Greenland AWS	3.56±1.79	6.23±1.49
Russia[a]		
Western Russia	78.5±105.5	232.6±117.92
Eastern Russia	49.55±42.83	79.14±40.3
Svalbard and Norway[a]		
Svalbard	12.83±5.27	5.22±2.76
Norway	25±8.49	42.32±8.07
North America[b]		
Pacific Northwest	52.5±69.24	35.36±57.61
Intermountain Northwest	34±21	8.97±6.05
North U.S. Plains	46.53±66.82	51.11±54.23
Canada	19.14±13.38	155.31±8.57
China[c]		
Qilian Mountains	–	305.09±230.19
Inner Mongolia	300.67±22.03	471.36±121.43
Northeast Industrial	1393.33±1082.05	2088.18±1229

[a] Doherty et al. (2010)

[b] Doherty et al. (2014)

[c] X. Wang et al. (2013)

Table S1. Comparison of observed and modeled snow surface black carbon concentration (C^{est}, ng g^{-1}). Observations are from Doherty et al. (2010), Wang et al. (2013), and Doherty et al. (2014), and model results are from the BRC simulation. Here, "AWS" indicates samples taken from Automatic Weather Sites. When more than one sample is present, we include ±1 standard deviation of the sample group. Missing model data indicates lack of snow cover in the simulation. Missing observation data from Quilan Mountains is due to near 0 BC mass concentration.

	Observations	NOBRC	BRC_PB	BRC
Canada and Alaska[a]				
Canadian Arctic	42.65±7.0	39.68±9.2	51.23±6.81	64.0±6.57
Canadian subarctic	42.54±5.79	36.32±16.4	43.57±12.83	52.65±9.78
N. Alaska Coast	53	19.88	39.23	56.25
Ellesmere Island	61	34.01	39.67	47.91
Greenland[a]				
South Greenland	33	–	–	–
Central Greenland	51	35.74	46.02	58.86
Northeast Greenland	45.33±16.2	–	–	–
Northwest Greenland	47	49.26	57.41	70.38
Greenland AWS	47.57±6.32	41.38±6.68	50.71±7.25	63.55±8.38
Russia[a]				
Western Russia	24.25±3.95	8.81±8.06	19.19±17.26	28.51±26.1
Eastern Russia	40.64±8.46	28.01±6.77	48.43±4.6	64.14±8.49
Svalbard and Norway[a]				
Svalbard	28.83±4.36	37.07±3.24	45.16±2.61	53.41±6.04
Norway	24±2.83	17.51±0.37	35.48±0.18	50.0±3.78
North America[b]				
Pacific Northwest	22.5±6.19	–	19.67±19.69	30.28±44.71
Intermountain Northwest	35.88±16.41	55.98±31.17	64.63±23.03	72.05±13.64
North U.S. Plains	61.88±22.05	48.58±41.3	57.21±29.23	62.55±15.13
Canada	47.29±13.85	24.66±29.4	37.59±21.61	44.71±15.94
China[c]				
Qilian Mountains	~100	–	8.57±0.93	21.5±4.68
Inner Mongolia	47.3±9.29	–	51.92±20.85	50.79±20.92
Northeast Industrial	30.33±8.5	–	1.87±1.28	4.37±0.63

[a] Doherty et al. (2010)
[b] Doherty et al. (2014)
[c] X. Wang et al. (2013)

Table S2. Comparison of observed and modeled fractional contribution to non-BC aerosol light absorption ($f_{est, \%}$). Observations are from Doherty et al. (2010), X. Wang et al. (2013), and Doherty et al. (2014). Here, "AWS" indicates samples taken from Automatic Weather Sites. Model simulations are described in Table 2, and model f_{est} is (OC SDE + dust SDE) / Total Aerosol SDE. When more than one sample is present, we include ±1 standard deviation of the sample group. Missing data indicate lack of snow cover in the model simulation or snow cover strongly darkened by BC leading to unphysical values for model SDE.

Region	Land Area (km^2)	Sea-Ice Area (km^2)	Sea-Ice / Land Area
Arctic	1.86×10^7	1.19×10^7	0.64
Antarctic	1.42×10^7	1.06×10^7	0.74

Table S3. Comparison of land and sea ice surface areas in the Arctic (60˚N–90˚N) and Antarctic (60˚S–90˚S) receptor regions (Fig. 7). Land area is calculated by multiplying land fraction by grid-cell surface area. Sea-ice fraction is calculated by multiplying grid-cell sea-ice percentages by grid-cell surface area (Figure S12).